Technium Vol. 31, pp.79-95 (2026)
ISSN: 2668-778X
www.techniumscience.com

A DFT Investigation of Alkali Metal Doping for the Tuning of Circumcoronene's Electronic Properties

Noora B. Shwayyea[1], Mohammed A. Khammat[1], Alaa M. Khudhair[1,2*]

[1]Department of Physics, College of Science, University of Sumer, Iraq, Thi-Qar 64000, Iraq

[2]Department of Physic, College of Science, University of Sfax, Tunisia, Sfax

[*]**Corresponding author:** mohammedali2001k@gmail.com

Abstract

In this study, the electronic and chemical reactivity properties of circumcoronene (CC), a graphene analog with significant potential for nanoelectronic applications, are examined in relation to the contamination of sodium and potassium. The research analyzes seven distinct structural configurations that involve a variety of doping schemes using density functional theory (DFT) at the B3LYP/6-31G level of theory. Energy gaps, Fermi levels, dipole moments, HOMO, LUMO, and density of states (DOS) are assessed as critical electronic parameters. The results indicate that alkali metal doping consistently reduces the band gap and improves conductivity. The most pronounced effect is seen in co-doping (Na and K), which reduces the band gap to 1.012 eV and increases the dipole moment and Fermi level. Enhanced reactivity and tunability were confirmed by the calculation of chemical indices, including ionization potential, electron affinity, hardness, softness, electronegativity, and electrophilicity, during the doping process. These results underscore the efficacy of Na and K incorporation as a strategic approach to alter the optoelectronic properties of circumcoronene, thereby confirming its suitability for future applications in advanced nanoelectronics devices.

Keywords: DFT, Circumcoronene, energy gap, DOS, electronic properties.

1. Introduction

Graphene is among the most extensively researched nanoscale materials concerning their electrical properties [1]. Graphene constitutes one of the most auspicious materials currently under investigation in this decade, owing to its extensive global potential and its capacity to enhance various domains and applications, thereby

elevating human existence to a higher echelon of civilization. Numerous scholars postulate that if the preceding century was characterized as the era of plastics (silicone), then this century appears poised to emerge as the epoch of grapheme [2]. Since the year 2004, there has been a significant escalation in the volume of scholarly publications pertaining to graphene, with the quantity of articles disseminated in academic journals surpassing 15,000 by the year 2014 [3]. Circumcoronene (CC), a substantial polycyclic aromatic hydrocarbon, possesses notable thickness attributed to its exceptional electrical, optical, and structural properties [4-8]. It is classified within the category of graphene analogs and, consequently, can be regarded as an exemplary framework for the examination of polymers exhibiting extended π-systems, thereby holding considerable importance in the domains of materials science and nanoelectronics. Its utility is notably recognized in the context of organic light-emitting diodes (OLEDs) [9, 10]. Due to their low toxicity, enduring photoluminescence, chemical stability, and significant quantum confinement effect, GQDs are acknowledged as a distinctive material for applications in biology, optoelectronics, energy, and the environment [11, 12]. The characteristics of quantum dots are fundamentally distinct from those of larger constructions composed of the same materials. Indeed, these nanostructures possess a remarkable capacity for tunability, which facilitates a broad spectrum of applications, including but not limited to semiconductor electronics, light-emitting diodes (LEDs), quantum computing, solar energy conversion, medical applications, bioimaging, oncological therapies, and plasmonic technologies, among others. Furthermore, the exceptionally high carrier mobility of graphene, coupled with its linear band dispersion, positions it favorably for various optoelectronic applications [13-16].

In the present investigation, we seek to illuminate the implications of incorporating sodium and potassium into the electronic characteristics of circumcoronene (CC). The objective is to examine the influence of these alterations on the electronic properties of (CC), thereby facilitating prospective advancements in the field of nanoelectronics.

2. Theoretical details

Gaussian 16 software package [17, 18]. The electrical characteristics of circumcoronene were examined utilizing both time-independent and time-dependent functional density (DFT) [19-22]. Employed in this study was the Density Functional Theory (DFT) methodology to examine the electronic characteristics pertaining to all seven structural configurations. Each of the seven carbon-carbon (CC) structures underwent optimization utilizing the unrestricted B3LYP functional in conjunction with the 6-31G basis set within the DFT framework [23-25].

The electronic properties of CC encompass the energy gap (E_{gap}), Fermi level (E_{FL}), energies of LUMO orbitals (E_{LUMO}), energies of HOMO orbitals (E_{HOMO}), and the resolution of the density of states (DOS). which encompasses the parameters of chemical reactivity, serves as a significantly valuable tool for the exploration of reactivity trends, excited states, and assessments of toxicity. These parameters comprise chemical hardness (η), chemical softness (S), chemical potential (μ), and the electrophilicity index (ω). The derivation of these parameters can be achieved through [26-28]:

$$\mu = -\frac{(IP + EA)}{2} \quad (1)$$

$$\eta = \frac{(IP - EA)}{2} \quad (2)$$

$$S = \frac{(IP - EA)}{2} \quad (3)$$

$$\omega = \frac{\mu^2}{2\eta} \quad (4)$$

The application of Koopman's theorem provides a method for approximating the ionization potential (IP) and the electron affinity (EA) [29-31]:

$$IP = -E_{HOMO} \quad (5)$$

$$EA = -E_{LUMO} \quad (6)$$

where E_{HOMO} and E_{LUMO} denote the energy states associated with the Highest Occupied Molecular Orbital (HOMO) and the Lowest Unoccupied Molecular Orbital (LUMO), respectively. Furthermore, we ascertain the electronic band gap as well as the Fermi level energy by employing the subsequent equation [32-34]:

$$E_g = E_{LUMO} - E_{HOMO} \quad (7)$$

$$E_{FL} = \frac{(E_{LUMO} + E_{HOMO})}{2} \quad (8)$$

To investigate the structural stability of CC following the addition of potassium and sodium, cohesion energies were computed for each structure. The structures with the greatest negative values are the most stable.

3. Results and discussions

This section provides a thorough investigation of the electrical and structural characteristics of circumcoronene ($C_{54}H_{18}$) and its alkali metal-doped derivatives through density functional theory (DFT). The examination encompasses virgins, singly doped, and co-doped configurations with sodium (Na) and potassium (K), evaluated via geometric optimization, HOMO-LUMO distributions, density of states (DOS), Fermi level, work function, and global chemical reactivity indices.

(a)

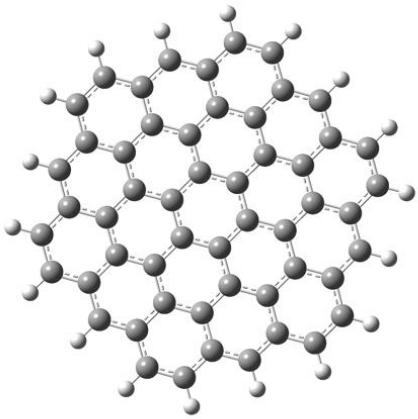

(b)

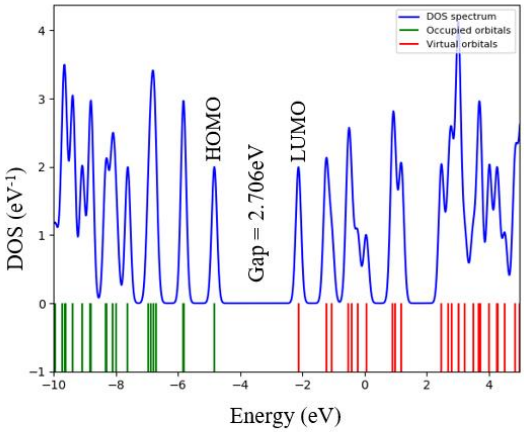

(c)

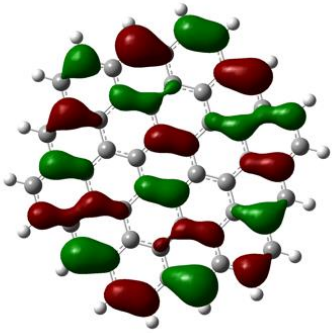

(d)

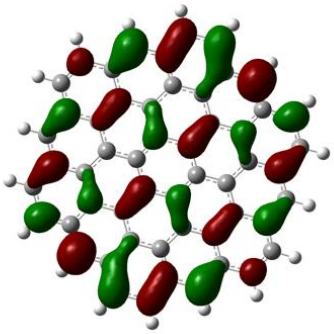

Fig. 1: (a) Geometric configuration of pure circumcuronine, (b) DOS, (c) HOMO, and (d) LUMO.

3.1.Pristine and Monometallic Doped Systems

The optimized geometry of the virgin circumcoronene molecule (Fig. 1a) displays a symmetric hexagonal configuration with uniformly distributed π-electrons throughout the aromatic system. The bond lengths are homogeneous and align with values anticipated for sp^2-hybridized carbon atoms, confirming structural stability. The electronic density of states (DOS) and orbital diagrams (Figs. 1b–d) indicate a HOMO-LUMO energy gap of 2.706 eV (as shown in Table 2), affirming its semiconducting characteristics and restricted chemical reactivity.

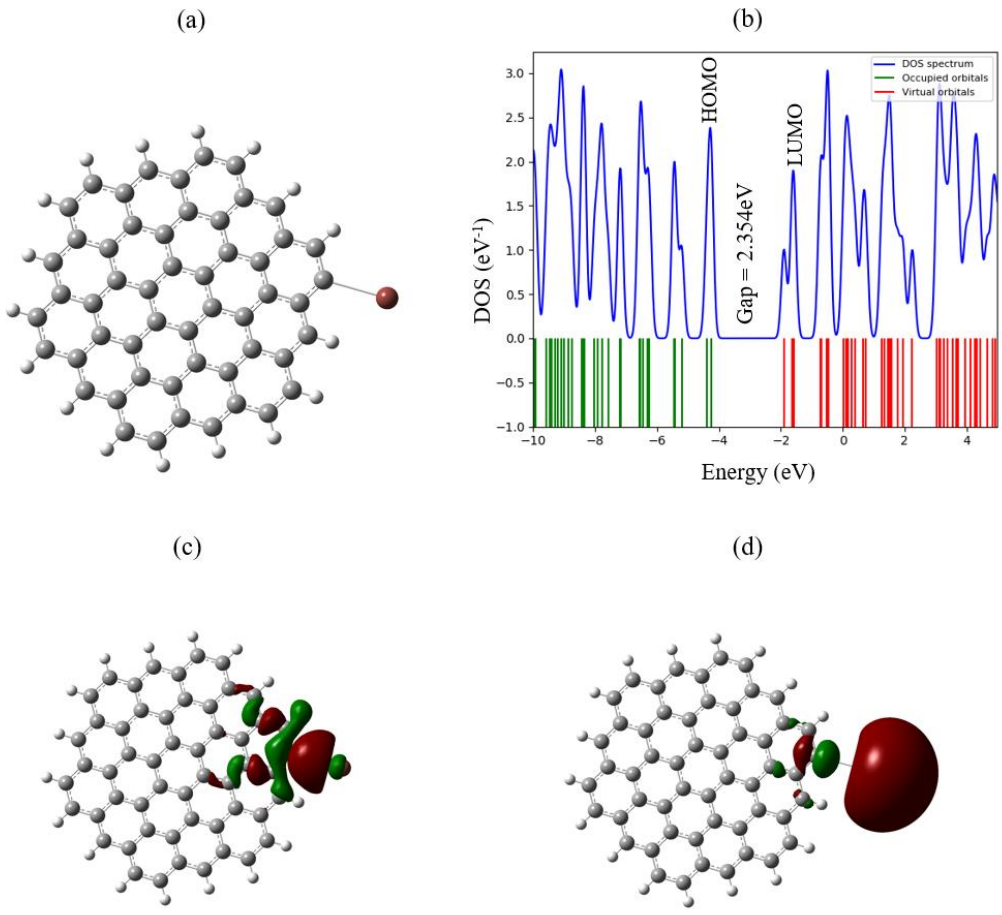

Fig. 2: (a) Geometric configuration of circumcuronine after addition (1K), (b) DOS, (c) HOMO, and (d) LUMO.

Doping with a solitary potassium atom (Fig. 2) induces a minor out-of-plane distortion, signifying localized charge transfer from the alkali metal to the carbon lattice. The band gap diminishes to 2.354 eV, and new mid-gap states emerge in the density of states, indicating an increased electronic density at the Fermi level. The HOMO and LUMO orbitals exhibit greater spatial localization at the dopant site, indicating a potential for enhanced interaction with external fields or chemical entities.

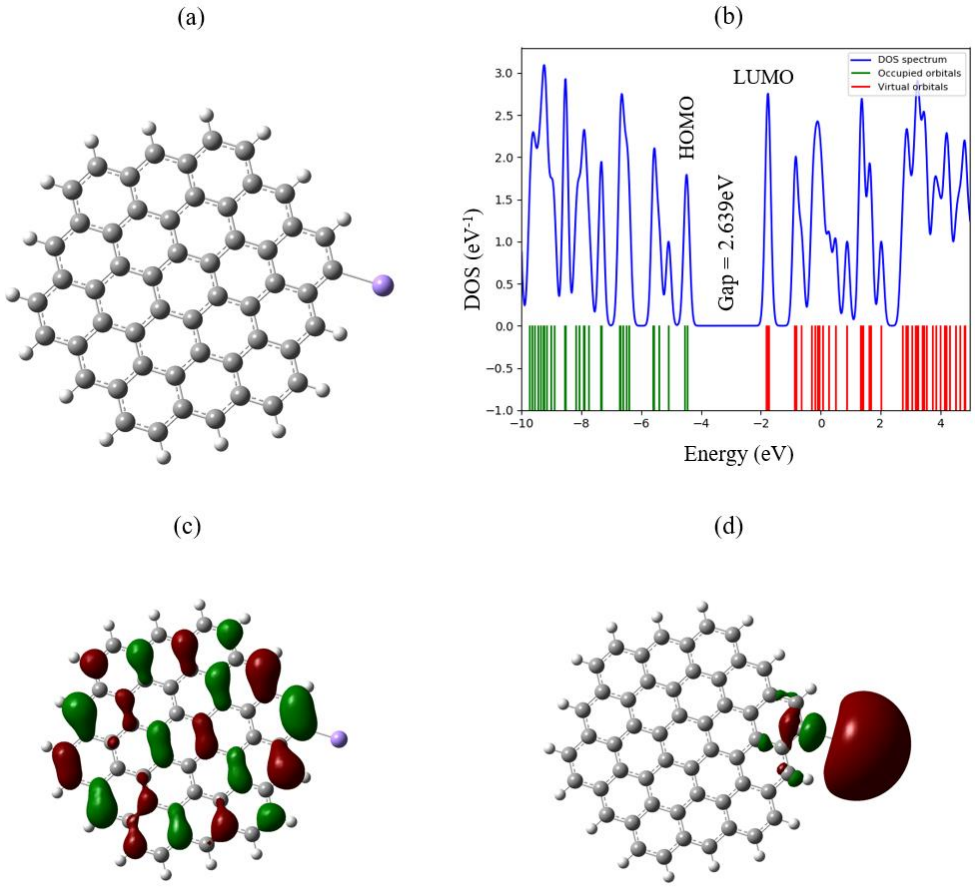

Fig. 3: (a) Geometric configuration of circumcuronine after addition (1Na), (b) DOS, (c) HOMO, and (d) LUMO

Doping with a sodium atom (Fig. 3) results in a marginally elevated band gap of 2.639 eV and more nuanced electrical alterations. In comparison to K, Na produces diminished DOS peaks and leads to a reduced Fermi level. Its elevated electronegativity results in a more modest polarization (dipole moment: 8.24 D compared to 12.35 D for K) and a diminished electron-donating impact. These complexes exhibit enhanced chemical softness compared to the pristine molecule, indicating improved reactivity while preserving modest electronic stability. These observations corroborate prior studies on alkali-metal doping in nanocarbon

systems, validating the influence of single-atom doping on band gap modulation and surface polarization.

This structural system contains a single Potassium (K) atom. The HOMO energy was seen to increase to -4.254 eV, compared to -4.831 eV for CC; and the LUMO energy was seen to increase to -1.900 eV, while the Eg was reduced to 2.354 eV; indicating an increased conductivity of the CC system. The Fermi-level was increased (E_{FL} = -2.846 eV) indicating an increased carrier concentration; and the calculated dipole moment (1.387 Debye) also increased indicating an increased charge asymmetry.

Figure 3 shows where we added a single sodium (Na) atom. The HOMO is at –4.442 eV and LUMO is at –1.802 eV, which gives Eg = 2.639 eV. The Eg is slightly larger than the K-doped case, but it is still smaller than the pure CC material Even when the Na atom is added, there is still a reduced energy gap compared to pure CC. The Fermi level is –3.122 eV and the dipole moment of the structure was 2.681 Debye, which would indicate moderate polarization.

3.2. Effects of Co-doping and Sensitivity to Configuration

The simultaneous introduction of Na and K atoms (Fig. 4) markedly modifies the DOS, resulting in a HOMO-LUMO gap reduction to 1.294 eV and an increase in the dipole moment to 15.62 D. The pronounced orbital asymmetry and distinct density of states peaks at the Fermi level indicate a material exhibiting quasi-metallic properties. These modifications signify enhanced electronic conductivity and the possibility for applications in charge transport and nanoelectronic devices. An isomeric co-doped arrangement (Fig. 5) illustrates the sensitivity of electrical behavior to the placement of dopants. Despite the stoichiometry being unchanged, the band gap rises to 2.038 eV, while the dipole moment diminishes to 4.42 D, signifying decreased reactivity and reestablished symmetry (as shown in Table (1,2)). The reduced asymmetry in the electronic structure results in less charge redistribution, rendering this form more electrically stable yet less reactive. Configurational dependence is essential for device engineering, as the spatial positioning of dopants offers a controlled variable for performance optimization.

Technium Vol. 31, pp.79-95 (2026)
ISSN: 2668-778X
www.techniumscience.com

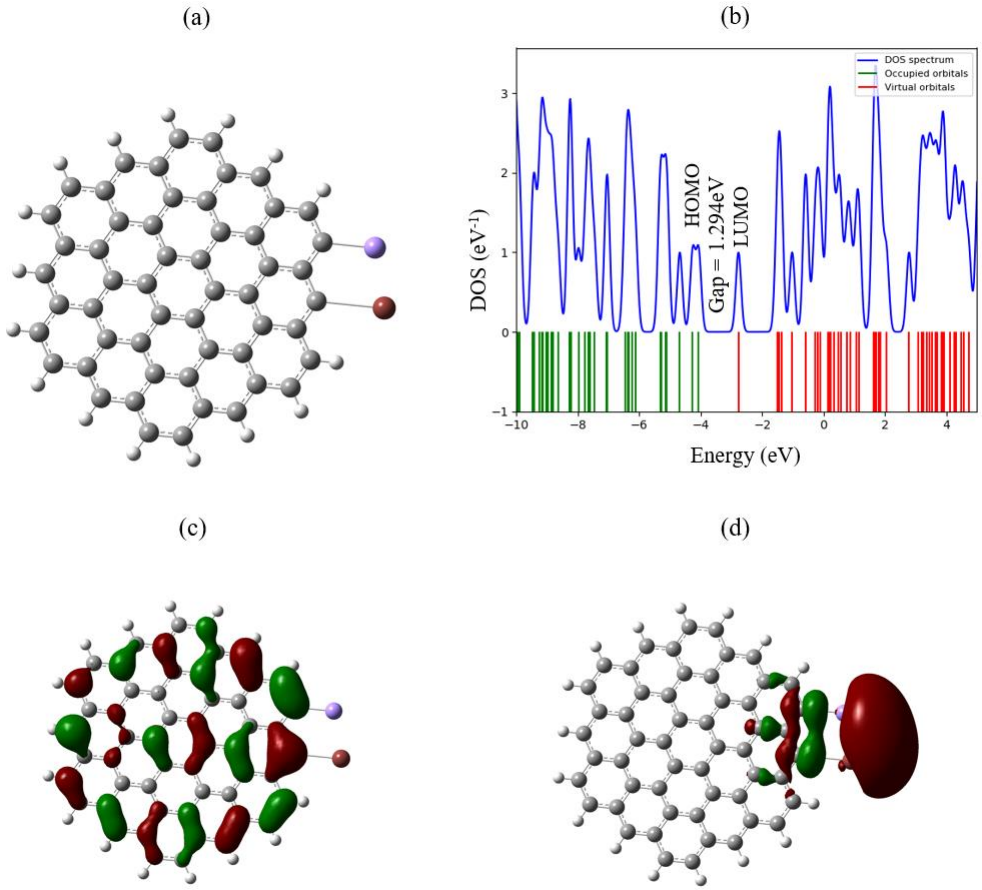

Fig 4: (a) Geometric configuration of circumcuronine after addition (1NA and 1K), (b) DOS, (c) HOMO, and (d) LUMO

Table 1: The values of the total energy (E_T), dipole moment (DM), Fermi level energy(E_{FL}) eV, work function ($\boldsymbol{\phi}$) eV.

Structure	$\boldsymbol{E_t}$	**DM**	$\boldsymbol{E_{fl}}$	$\boldsymbol{\phi}$
CC	-56299.584	0.010	-3.478	3.478
K-CC	-72592.593	12.35	-3.077	3.077
Na-CC	-60684.657	8.246	-3.122	3.122
Na_1K_1-CC (Fig. 5)	-76990.370	15.62	-3.417	3.417
Na_1K_1-CC (Fig. 6)	-76991.486	4.425	-2.802	2.802
Na_2K_2-CC (Fig. 7)	-97694.808	1.792	-2.973	2.973
Na_2K_2-CC (Fig. 8)	-97696.811	0.001	-2.399	2.399

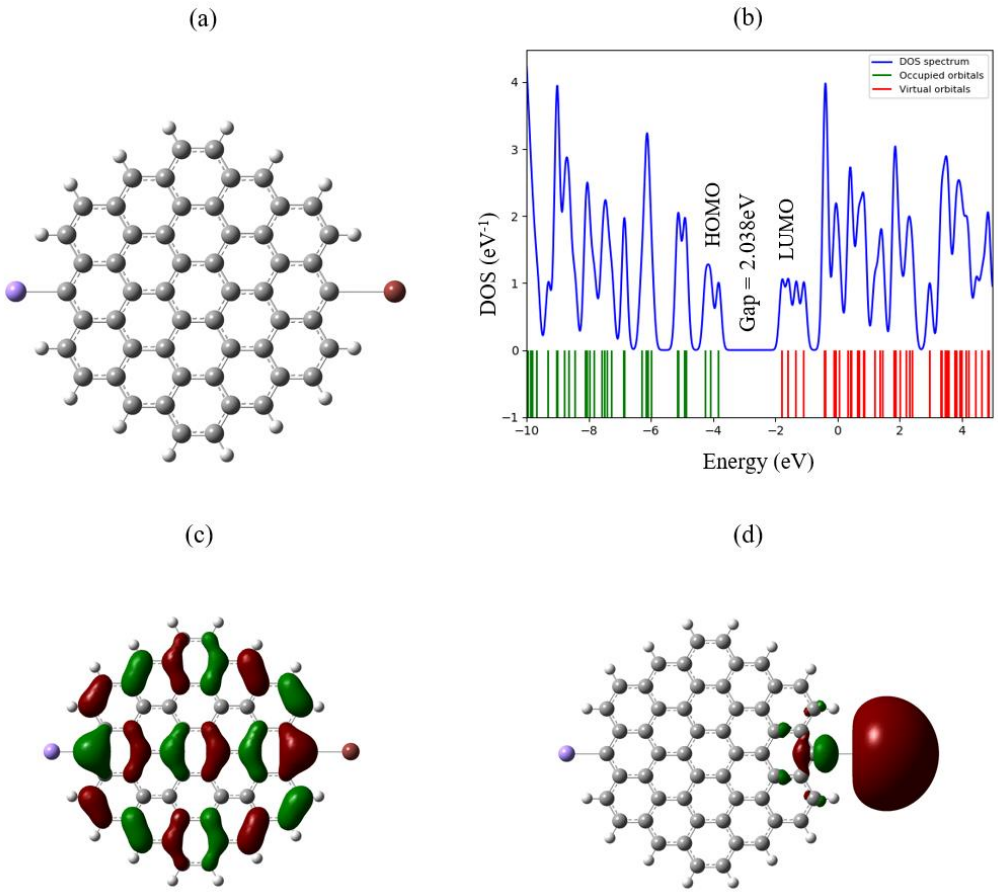

Fig. 5: (a) Geometric configuration of circumcuronine after addition (1Na and 1K) in various locations, (b) DOS, (c) HOMO, and (d) LUMO.

3.3. High-Concentration Co-Doped Configurations

Additional doping with two sodium and two potassium atoms (Fig. 6) amplifies these effects, yielding the lowest recorded band gap of 1.012 eV (see Table 2) and considerable density of states around the Fermi level. The HOMO and LUMO exhibit significant localization around the dopants, signifying increased conductivity and heightened chemical sensitivity. These systems demonstrate significant asymmetry and polarization, shown by high dipole moments, suggesting their appropriateness for field-responsive or catalytically active settings [35].

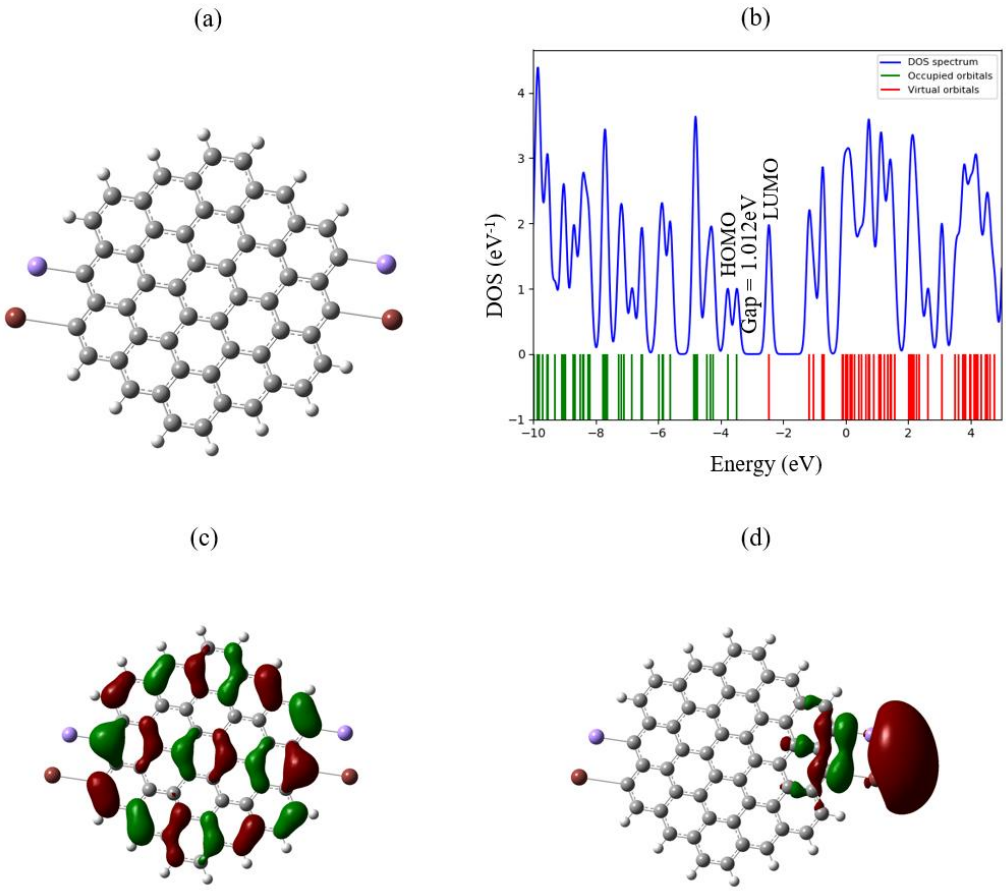

Fig. 6: (a) Geometric configuration of circumcuronine after addition (2Na and 2K), (b) DOS, (c) HOMO, and (d) LUMO

In a structural version (Fig. 7) with the same composition but altered dopant arrangement, the gap rises to 1.751 eV while the dipole moment nears zero. The symmetric arrangement electrically stabilizes the system and diminishes polarizability. This structure, although less reactive, may be preferable in applications necessitating long-term chemical and thermal durability. These findings illustrate how the concentration and spatial arrangement of dopants can be utilized to modify the electrical and chemical properties of circumcoronene, facilitating the tailored creation of material attributes [36].

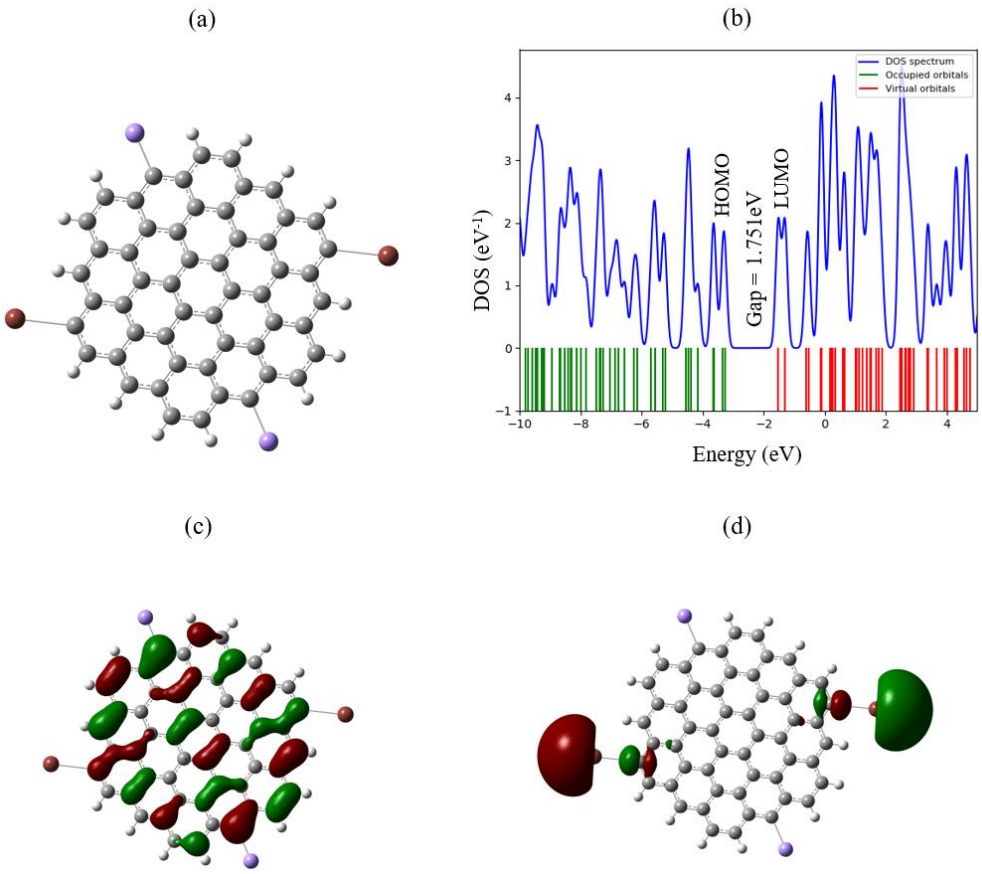

Fig. 7: (a) Geometric configuration of circumcuronine after addition (2Na and 2K) in various locations, (b) DOS, (c) HOMO, and (d) LUMO.

3.4. Descriptors of Reactivity

Table 1 aggregates information on total energy, dipole moments, Fermi levels, and work functions. A discernible pattern is noted: doped systems have reduced work functions and increased Fermi levels, indicating improved surface electron mobility. The substantial decrease in work function (from 3.478 eV in the pristine system to as low as 2.399 eV) indicates enhanced electron emission efficiency, advantageous for applications such as electron emitters and field-effect transistors [21, 37, 38].

The bar chart (Fig. 9) depicts the fluctuations in energy gap and work function for both pristine and alkali-metal-doped circumcoronene structures. A significant decrease in band gap is seen with Na and K doping, with the lowest value (1.012 eV) recorded in the Na_2K_2-CC (Fig. 7), signifying improved electrical conductivity. Similarly, the work function diminishes with doping, reaching a low of 2.399 eV in Na_2K_2-CC (Fig. 8), indicating enhanced electron emission capability. The findings

validate that the electrical characteristics of circumcoronene may be efficiently adjusted by alkali metal integration and dopant arrangement.

Table 2: The values of the E_{HOMO} , E_{LUMO}, energy gap (E_{gap}) for all structures in eV unit.

Structure	E_{HOMO}	E_{LUMO}	E_g
CC	-4.831	-2.126	2.706
K-CC	-4.254	-1.900	2.354
Na-CC	-4.442	-1.803	2.639
Na_1K_1-CC (Fig. 5)	-4.064	-2.770	1.294
Na_1K_1-CC (Fig. 6)	-3.821	-1.783	2.038
Na_2K_2-CC (Fig. 7)	-3.479	-2.467	1.012
Na_2K_2-CC (Fig. 8)	-3.274	-1.523	1.751

Table 3 enumerates global reactivity descriptors: ionization potential (IP), electron affinity (EA), hardness (η), softness (S), electronegativity (μ), and electrophilicity (ω). Co-doped systems, specifically $C_{54}H_{14}Na_2K_2$, exhibit low hardness, high softness, and pronounced electrophilic properties, rendering them excellent candidates for catalytic and sensing applications. The enhancement in softness is associated with an improved capacity to donate or take electrons when interacting with target molecules, a crucial characteristic of sensor materials. The electrophilicity index further confirms that these complexes may function as potent electron acceptors [39]. Systems with elevated ω values typically exhibit favorable interactions with nucleophilic species, providing a customizable framework for surface chemistry and tailored functionalization [40].

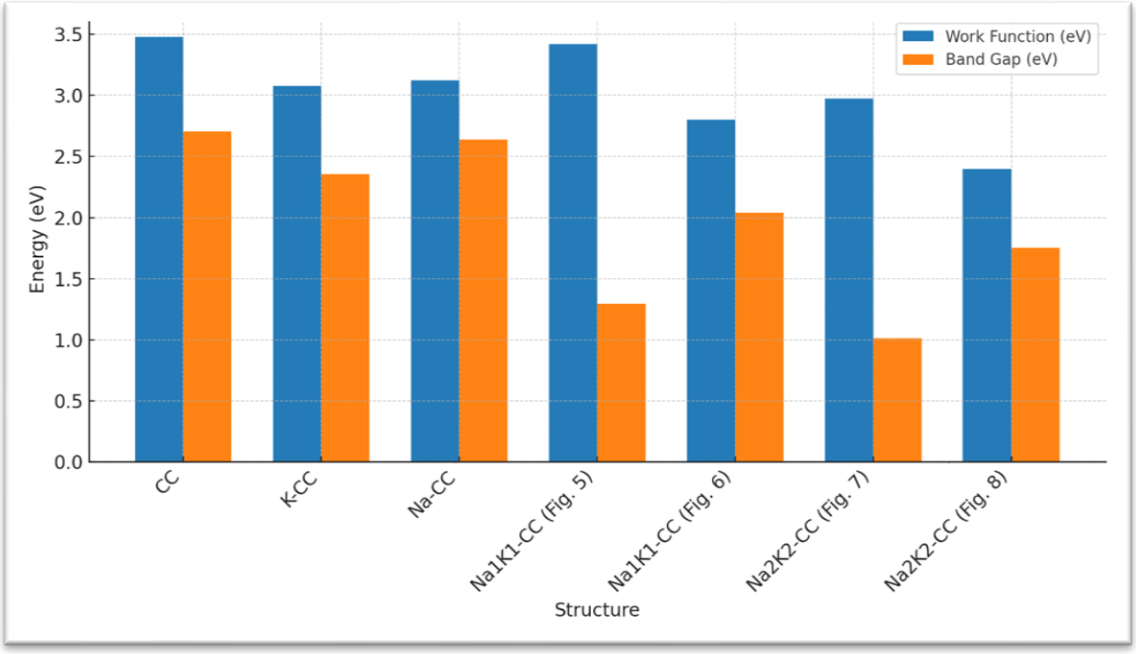

Fig. 9: Comparison of energy gaps and work function of all structures.

Table 3: All chemical indices were calculated, including the ionization potential (IP), electron affinity (EA), hardness (H), softness (S), and electronegativity (μ) and electrophilicity (ω), in (eV) unit.

Structure	IP	EA	H	S	μ	ω
CC	4.831	2.126	1.353	0.3696	4.472	3.478
K-CC	4.254	1.900	1.177	0.425	4.021	3.077
Na-CC	4.442	1.803	1.320	0.379	3.694	3.122
Na_1K_1-CC (Fig. 5)	4.064	2.770	0.647	0.773	9.019	3.417
Na_1K_1-CC (Fig. 6)	3.821	1.783	1.019	0.491	3.852	2.802
Na_2K_2-CC (Fig. 7)	3.479	2.467	0.506	0.988	8.736	2.973
Na_2K_2-CC (Fig. 8)	3.274	1.523	0.875	0.571	3.286	2.399

The findings validate that alkali metal doping is an efficacious method for modifying the electronic structure, reactivity, and stability of circumcoronene. This study emphasizes the capability of dopant-driven modulation to tailor material performance, offering a solid theoretical basis for the development of high-efficiency nanodevices in electronics, sensing, and energy storage technologies [4].

4. Conclusion

This study utilized DFT-based simulations to systematically examine the electrical structure, chemical reactivity, and structural modification of both pristine and alkali-metal-doped circumcoronene complexes. The findings indicate that both the nature and arrangement of dopants substantially affect critical parameters like band gap, Fermi level, dipole moment, and global reactivity indices. Single-atom doping with sodium or potassium results in substantial band gap reduction and enhanced dipole polarization, with potassium demonstrating a more pronounced electrical effect than sodium. Co-doping configurations result in significant alterations, such as considerable band gap reduction, orbital localization, and asymmetric charge distribution. The effects are further amplified in high-concentration co-doped systems, which exhibit exceptional tunability of their electrical characteristics and promise for multifunctional applications.

Co-doped structures demonstrate increased softness and electrophilicity from a reactivity standpoint, affirming their appropriateness for catalytic, sensing, or charge-transfer applications. The configurational dependence of electrical behavior indicates that meticulous spatial control of dopant placement is crucial for enhancing device performance.

Ethical Approval

This research did not contain any studies involving animal or human participants, nor did it take place on any private or protected areas. No specific permissions were required for corresponding locations.

Declaration of Competing Interest

The authors declare that they have no conflict of interest.

Authors contributions

Alaa M. Khudhair and other authors participated in finding and interpreting the results and writing and commenting on the manuscript.

Research data

No data was used for the research described in the article.

Funding

This study received no support from governmental, commercial, or not-for-profit funding entities.

Availability of data and materials

Data sharing is not relevant to this article since no new data was produced or analyzed in this investigation.

References

[1] M. H. Al-Abboodi, F. N. Ajeel, and A. M. Khudhair, "Influence of oxygen impurities on the electronic properties of graphene nanoflakes," *Physica E: Low-dimensional Systems and Nanostructures,* vol. 88, pp. 1-5, 2017.

[2] A. H. C. Neto, "The carbon new age," *Materials today,* vol. 13, no. 3, pp. 12-17, 2010.

[3] S. Ahn, J. Sung, H. Kim, and Y. Sung, "Emerging analysis on the preparation and application of graphene by bibliometry," *Journal of Material Sciences & Engineering,* vol. 4, no. 192, pp. 2169-0022.2015 ,

[4] R. Geetha Sadasivan Nair, A. K. Narayanan Nair, and S. Sun, "Density functional theory study of doped coronene and circumcoronene as anode materials in lithium-ion batteries," *Scientific Reports,* vol. 14, no. 1, p. 15220, 2024.

[5] A. M. Khudhair and A. B. Ahmed, "Utilizing circumcoronene and BN circumcoronene for the delivery and adsorption of the anticancer drug floxuridine," *Computational and Theoretical Chemistry,* vol. 1222, p. 114075, 2023.

[6] M. Malček and M. N. D. Cordeiro, "A DFT and QTAIM study of the adsorption of organic molecules over the copper-doped coronene and circumcoronene," *Physica E: Low-dimensional Systems and Nanostructures,* vol. 95, pp. 59-70, 2018.

[7] N. Balbool, M. K. Salman, A. M. Khudhair, and F. N. Ajeel, "Study the Effect of Phosphorous Impurities on Electronic and Optical Properties of Circumcoronene via DFT investigations," *Sumer Journal for Pure Science,* vol. 3, no. 2, 2024.

[8] W. Zeng and J. Wu, "Open-shell graphene fragments," *Chem,* vol. 7, no. 2, pp. 358-3.2021 ,86

[9] L. De Souza, G. M. de Castro, L. Marques, and J. Belchior, "A DFT investigation of lithium adsorption on graphenes as a potential anode material in lithium-ion batteries," *Journal of Molecular Graphics and Modelling,* vol. 108, p. 107998, 202.1

[10] L. A. Ponomarenko *et al.*, "Chaotic Dirac billiard in graphene quantum dots," *Science,* vol. 320, no. 5874, pp. 356-358, 2008.

[11] Y. R. Kumar, K. Deshmukh, K. K. Sadasivuni, and S. K. Pasha, "Graphene quantum dot based materials for sensing, bio-imaging and energy storage applications: a review," *RSC advances,* vol. 10, no. 40, pp. 23861-23898, 2020.

[12] T. D. Thangadurai, N. Manjubaashini, D. Nataraj, V. Gomes, and Y. I. Lee, "A review on graphene quantum dots, an emerging luminescent carbon nanolights: Healthcare and Environmental applications," *Materials Science and Engineering: B,* vol. 278, p. 115633, 2022.

[13] Z. Jin, P. Owour, S. Lei, and L. Ge, "Graphene, graphene quantum dots and their applications in optoelectronics," *Current Opinion in Colloid & Interface Science,* vol. 20, no. 5-6, pp. 439-453, 2015.

[14] X. Chen *et al.*, "Graphene hybrid structures for integrated and flexible optoelectronics," *Advanced Materials,* vol. 32, no. 27, p. 1902039, 2020.

[15] X. Li, J. Yu, S. Wageh, A. A. Al-Ghamdi, and J. Xie, "Graphene in photocatalysis: a review," *small,* vol. 12, no. 48, pp. 6640-6696, 2016.

[16] S. Sagadevan *et al.*, "Functionalized graphene-based nanocomposites for smart optoelectronic applications," *Nanotechnology Reviews,* vol. 10, no. 1 ,pp. 605-635, 2021.

[17] F. N. Ajeel, M. H. Mohammed, and A. M. Khudhair, "Electronic, thermochemistry and vibrational properties for single-walled carbon nanotubes," *Nanoscience & Nanotechnology-Asia,* vol. 8, no. 2, pp. 233-239, 2018.

[18] A. M. Khudhair ,K. H. Bardan, A. Almusawe, and F. N. Ajeel, "Enhancement the electronic and optical properties for the dye Disperse Orange 13 and using in the solar cell device," in *IOP Conference Series: Materials Science and Engineering*, 2020, vol. 928, no. 7: IOP Publishing, p. 072031 .

[19] A. D. Laurent and D. Jacquemin, "TD-DFT benchmarks: a review," *International Journal of Quantum Chemistry,* vol. 113, no. 17, pp. 2019-2039, 2013.

[20] S. Idrissi, H. Labrim, L. Bahmad, and A. Benyoussef, "DFT and TDDFT studies of the new inorganic perovskite CsPbI3 for solar cell applications," *Chemical Physics Letters,* vol. 766, p. 138347, 2021.

[21] A. M. Khudhair and A. Ben Ahmed, "Pure and stone-wales defect armchair boron nitride graphene nanoribbons as anticancer drug delivery vehicles: a theoretical investigation," *Journal of Cluster Science,* vol. 35, no. 2, pp. 451-460, 2024.

[22] A. M. Khudhair and A. B. Ahmed, "The present and doped bilayer circumcoronene and bilayer BN circumcoronene as carriers for hydroxyurea anticancer drug delivery," *BioNanoScience,* vol. 14, no. 3, pp. 2976-2992, 2024.

[23] M. H. Mohammed, F. N. Ajeel, and A. M. Khudhair, "Analysis the electronic properties of the zigzag and armchair single wall boron nitride nanotubes with single Li impurity in the various sites," *Journal of Electron Spectroscopy and Related Phenomena,* vol. 228, pp. 20-24, 2018.

[24] A. Alrikabi, "Theoretical study of the design dye-sensitivity for usage in the solar cell device," *Results in physics,* vol. 7, pp. 4359-4363, 2017.

[25] M. A. Khammat, A. M. Khudhair, and N. B. Shwayyea, "Tailoring Electronic, Optical, and Reactive Properties of Br-and F-Doped Graphene Nanoflakes: A DFT-Based Study," *Materials Today Quantum,* p. 100048, 2025.

[26] A. Narita, X.-Y. Wang, X. Feng, and K .Müllen, "New advances in nanographene chemistry," *Chemical Society Reviews,* vol. 44, no. 18, pp. 6616-6643, 2015.

[27] A. M. Khudhair, M. H. Mohammed, F. N. Ajeel, and S. H. Mohammed, "Enhancement the electronic and optical properties of the graphene nanoflakes in the present S impurities," *Chemical Physics Impact,* vol. 6, p. 100154, 2023.
[28] A. M. Khudhair, A. B. Ahmed, F. N. Ajeel, and M. H. Mohammed, "Theoretical investigation on the therapeutic applications of C2B and C2O as targeted drug delivery systems for hydroxyurea and 6-thioguanine in cancer treatment," *Nano-Structures & Nano-Objects,* vol. 38, p. 101135, 2024.
[29] U. Bozkaya, "The extended Koopmans' theorem for orbital-optimized methods: Accurate computation of ionization potentials," *The Journal of Chemical Physics,* vol. 139, no. 15, 2013.
[30] A. M. Khudhair, A. Ben Ahmed, and F. N. Ajeel, "Computational Investigation of 6-Thioguanine Adsorption on Armchair Graphene Nanoribbons for Targeted Drug Delivery: Orientation-Dependent Stability ,Electronic Structure, and Delivery Efficiency," *The Journal of Physical Chemistry C,* vol. 129, no. 37, pp. 16593-16603, 2025.
[31] A. M. Khudhair, I. Dhouib, F. N. Ajeel, A. B. Ahmed, and B. Khemakhem, "A Novel Al8N8 and B8N8 Nanoring Monolayer for Sensing and Drug Delivery of Cisplatin and Nitrosourea Anticancer Drugs: A DFT Insight," *Journal of Inorganic and Organometallic Polymers and Materials,* pp. 1-14, 2025.
[32] D. D. Y. Setsoafia, K. S. Ram, H. M. Rad, D. Ompong, V. Murthy, and J. Singh, "DFT and TD-DFT calculations of orbital energies and photovoltaic properties of small molecule donor and acceptor materials used in organic solar cells," *Journal of Renewable Materials,* vol. 10, no. 10, pp. 2553-2567, 2022.
[33] A. M. Khudhair and H. A. Dhahi, "Adsorption properties and sensing capabilities of pristine and Stone–Wales defected BN nanosheets for lung cancer VOC biomarkers: A DFT investigation," *Chinese Journal of Physics,* 2025.
[34] A. M. Khudhair and A. Ben Ahmed, "Adsorption characteristics of the anticancer drug hydroxyurea with armchair BN graphene nanoribbons containing and lacking vacancy defects: insight via DFT calculations," *Journal of Superconductivity and Novel Magnetism,* vol. 37, no. 8, pp. 1509-1518, 2024.
[35] T. E. Gber *et al.*, "Retracted Article: Heteroatoms (Si, B, N, and P) doped 2D monolayer MoS 2 for NH 3 gas detection," *RSC advances,* vol. 12, no. 40, pp. 25992-26010, 2022.
[36] H. Asadi, K. Zhour, and A. Zavartorbati, "DFT study of Benzene, Coronene and Circumcoronene as zigzag graphene quantum dots," *Journal of Interfaces, Thin Films, and Low dimensional systems,* vol. 3, no. 1, pp. 203-210, 2019.
[37] J. Wen, J. Xie, X. Chen, and X. Li, "A review on g-C3N4-based photocatalysts," *Applied surface science,* vol. 391, pp. 72-123.2017 ,
[38] A. M. Khudhair, I. Dhouib, A. B. Ahmed, F. N. Ajeel, and B. Khemakhem, "DFT-based insights into cisplatin drug adsorption on transition metal dichalcogenides: toward targeted drug delivery systems," *Chinese Journal of Physics,* 2025.
[39] T. Abbaz, A. Bendjeddou, and D. Villemin, "Molecular orbital studies (hardness, chemical potential, electro negativity and electrophilicity) of TTFs conjugated between 1, 3-dithiole," *Int. J. Adv. Res. Sci. Eng. Technol,* vol. 5, no. 2, pp. 5150-5161, 2018.
[40] L. R. Domingo, M. Ríos-Gutiérrez, and P. Pérez, "Applications of the conceptual density functional theory indices to organic chemistry reactivity," *Molecules,* vol. 21, no. 6, p. 748, 2016.